

Functional Analysis

Shearlet based regularisation in statistical inverse learning
with an application to X-Ray tomography

A presentation by group code :-- FuncGrpEEEECS

Group Members

1. Shlok Mehendale (2022B4A71426G)
2. Anshul Jawale (2022B4A70075G)
3. Arjun Pardal (2022B4A70771G)
4. Aadi Joshi (2022B4A30315G)
5. Sparsh Upadhyaya (2022B4A31042G)



Shearlets are directional extensions of wavelets, generated by **scaling**, **shearing**, and **translating** a function in $L^2(\mathbb{R}^2)$, and are used to detect edges and boundaries in images.

Definition

Representation of a 2D Shearlet

Formula :-- $\psi_{a,s,t}(x) = a^{-\frac{3}{4}}\psi(A_a^{-1}S_s^{-1}(x - t))$

Key parameters

- $a > 0$ is the *scaling parameter*
- $s \in \mathbb{R}$ is the *shearing parameter*
- $t \in \mathbb{R}^2$ is the *translation parameter*
- A_a and S_s are *scaling matrix & shearing matrices*.

Parabolic scaling matrix which is used to stretch the function anisotropically (Length $\propto a$, Width $\propto a^{1/2}$).

$$A_a = \begin{pmatrix} a & 0 \\ 0 & a^{1/2} \end{pmatrix}$$

$$S_s = \begin{pmatrix} 1 & s \\ 0 & 1 \end{pmatrix}$$

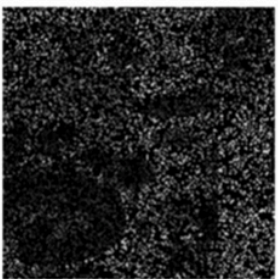
Shear matrix which is used to tilt the function without rotation.

 **Fun Fact** :-- the scaling factor is not random — it's perfectly tuned to keep the **energy** (or total "power") of the **shearlet constant** across all scales and directions!

Applications of Shearlet transform



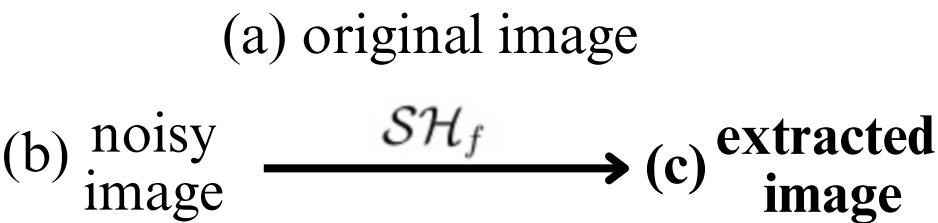
(a)



(b)



(c)



Shearlets and Regularization

Shearlet Transform

The associated *continuous Shearlet transform* of some $f \in L^2(\mathbb{R}^2)$ is given by

$$SH_f : \mathbb{R}^+ \times \mathbb{R} \times \mathbb{R}^2 \rightarrow \mathbb{C}, \quad SH_f(a, s, t) = \langle f, \psi_{ast} \rangle.$$

Co-orbit spaces

$$\mathcal{H}_{1,\omega} = \{f \in L^2(\mathbb{R}^d) : SH_\psi(f) \in L^1_\omega(\mathbb{S})\}$$

Shearlet Group

The (full) *shearlet group* \mathbb{S} is the set $\mathbb{R}^* \times \mathbb{R}^{d-1} \times (\mathbb{R} \times \mathbb{R}^{d-1})$ with the group operation


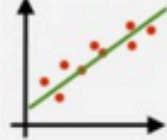
$$(a, s, t) \circ_{\mathbb{S}} (a', s', t') := (aa', s + |a|^{1-\gamma}s', t + S_s A_{a,\gamma} t').$$

Shearlet based regularisation

We now want to extend theorem 3.3 so that it can be applied to the more general framework of frames, rather than bases, which would allow in particular to consider **shearlet**-based regularization. This amounts to consider the following regularizer:

$$R(f) := \frac{1}{p} \sum_{\lambda \in \Lambda} m_\lambda^p |\langle f, \psi_\lambda \rangle|^p, \tag{36}$$

Definition The intersection of inverse problems [recovering an unknown function from an indirect, noisy measurements] and statistical learning [estimating functions from sampled, noisy data] is called **Statistical inverse Learning**

Inverse problem	vs	Statistical learning
$y = Af + w$  $\underset{\text{def.}}{A^T y} = \underset{\text{def.}}{(A^T A)} f + \underset{\text{def.}}{A^T w}$ $\underset{\text{def.}}{u} \quad \quad \quad \underset{\text{def.}}{C} \quad \quad \quad \underset{\text{def.}}{r}$		$y = Xf + \varepsilon$  $\underset{\text{def.}}{\frac{1}{n} X^T y} = \underset{\text{def.}}{\frac{1}{n} (X^T X)} f + \underset{\text{def.}}{\frac{1}{n} X^T \varepsilon}$ $\underset{\text{def.}}{u_n} \quad \quad \quad \underset{\text{def.}}{C_n} \quad \quad \quad \underset{\text{def.}}{r_n}$ $\downarrow \quad n \rightarrow +\infty \quad \downarrow \quad (x_i, y_i)_i \text{ i.i.d.}$ $\underset{\text{def.}}{u} = \mathbb{E}(yx) \quad \quad \quad \underset{\text{def.}}{C} = \mathbb{E}(xx^T)$
Regularized inversion: $\min_f \frac{1}{2} \ Af - y\ ^2 + \lambda \ f\ ^2$ $f_\lambda = (C + \lambda \text{Id}_p)^{-1} u$		Empirical risk minimization: $\min_f \frac{1}{2n} \ Xf - y\ ^2 + \lambda \ f\ ^2$ $f_{\lambda,n} = (C_n + \lambda \text{Id}_p)^{-1} u_n$
Exact covariance C	↔	Noisy covariance C_n
Deterministic bounded noise r	↔	Random noise r_n
Noise level $\varepsilon \stackrel{\text{def.}}{=} \ r\ $	↔	Noise level $\ r_n\ \sim \varepsilon = n^{-\frac{1}{2}}$




Preliminaries

(Inverse problem) given the noisy measurements $g^\delta : g^\delta = Af + \varepsilon$, recover f

(Statistical learning problem) given a sample $\{(u_n, v_n)\}_{n=1}^N : v_n = g(u_n) + \varepsilon_n$, recover g

(Statistical inverse learning problem) given $\{(u_n, v_n)\}_{n=1}^N : v_n = (Af)(u_n) + \varepsilon_n$, recover f

What we are trying to do?

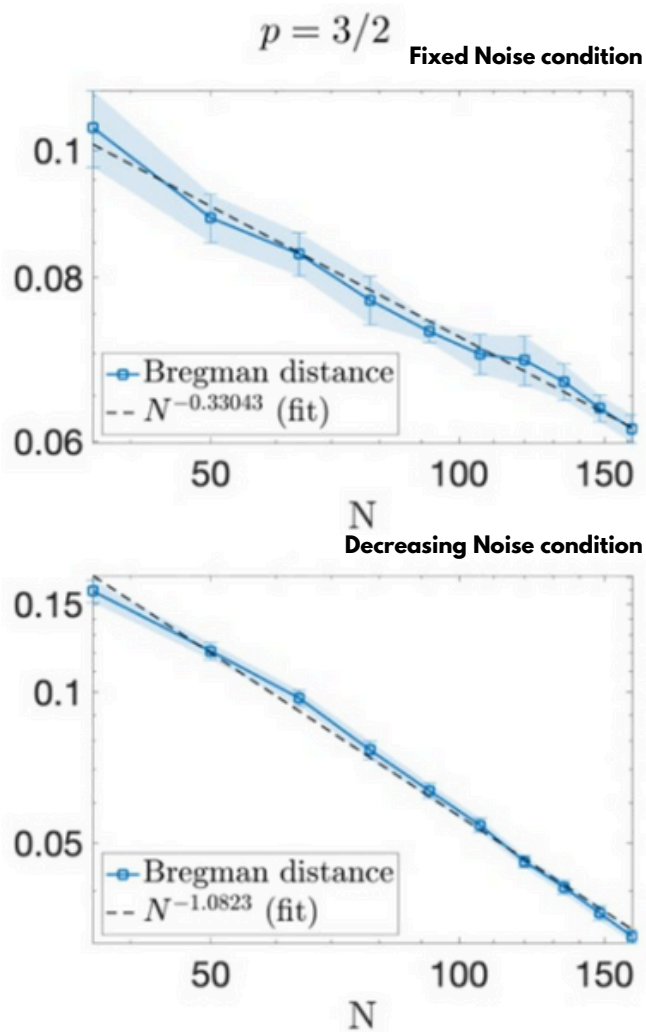


- ✓ Detecting edges using Haar wavelet transform
- ✓ Image 2 has ~80% of pixels missing
- ✓ Image 3 reconstructs the missing edges from image 2

Regularization is a technique in machine learning that adds a penalty to the model's loss function to discourage overfitting by limiting model complexity thus improving the generalisability of the model.

Definition

Bregman distance



Inferences from the plot

• If $\delta N \rightarrow \infty$ (and $\delta^2/N \rightarrow 0$), then

$$\mathbb{E} [D_R(f_{\alpha,N}^\delta, f^\dagger)] \lesssim \left(\frac{\delta^2}{N}\right)^{\frac{1}{p}} \text{ for } \alpha \simeq \left(\frac{\delta^2}{N}\right)^{\frac{1}{p}};$$

Theorem 2.4 (Theorem 4.3, [7]). The regularized solution $f_{\alpha,N}^\delta$ given by (2) satisfies the following inequality:

$$D_R(f_{\alpha,N}^\delta, f^\dagger) \leq \tilde{C}_p \left[\gamma_1^{-q} \mathcal{R}(\alpha \gamma_1^q, \mathbf{u}; f^\dagger) + H(\alpha, \delta, \gamma_1, \gamma_2) R^*(A_\delta^* \epsilon_N) + \left(\gamma_1^p + \frac{\gamma_2^p}{\alpha} \right)^{\frac{1}{p-1}} R(f^\dagger) \right] \quad (11)$$

for arbitrary $\gamma_1, \gamma_2 > 0$, where $\tilde{C}_p > 0$ is a constant dependent on p, q is the Hölder conjugate of p and

$$H(\alpha, \delta, \gamma_1, \gamma_2) = \frac{\delta^q}{\alpha \gamma_2^q} + \left(\gamma_1^p + \frac{\gamma_2^p}{\alpha} \right)^{\frac{1}{p-1}} \left(\frac{\delta}{\alpha} \right)^q. \quad (12)$$

• If δN is bounded, then

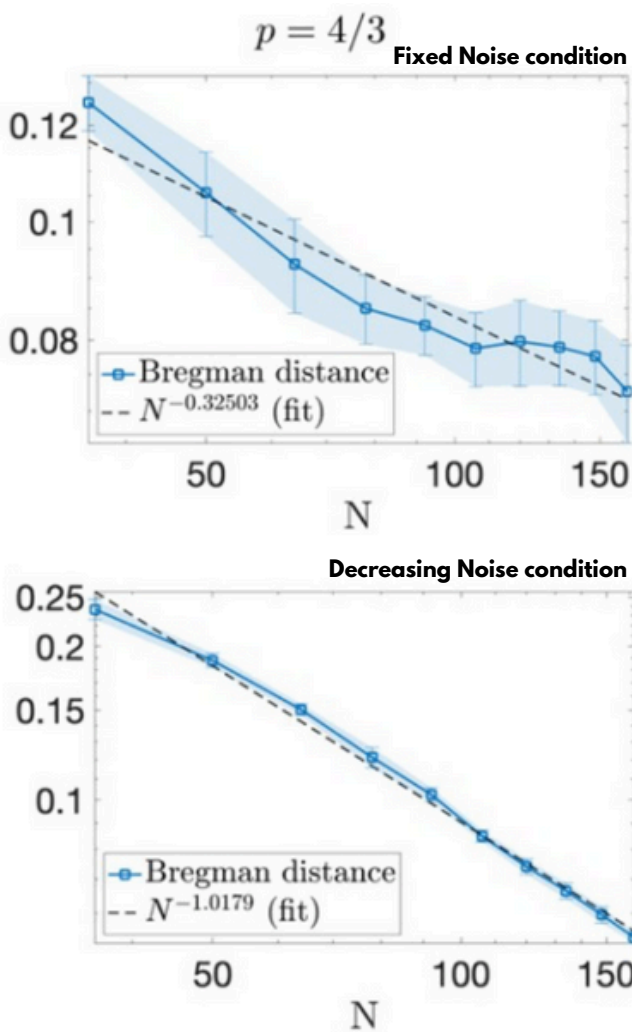
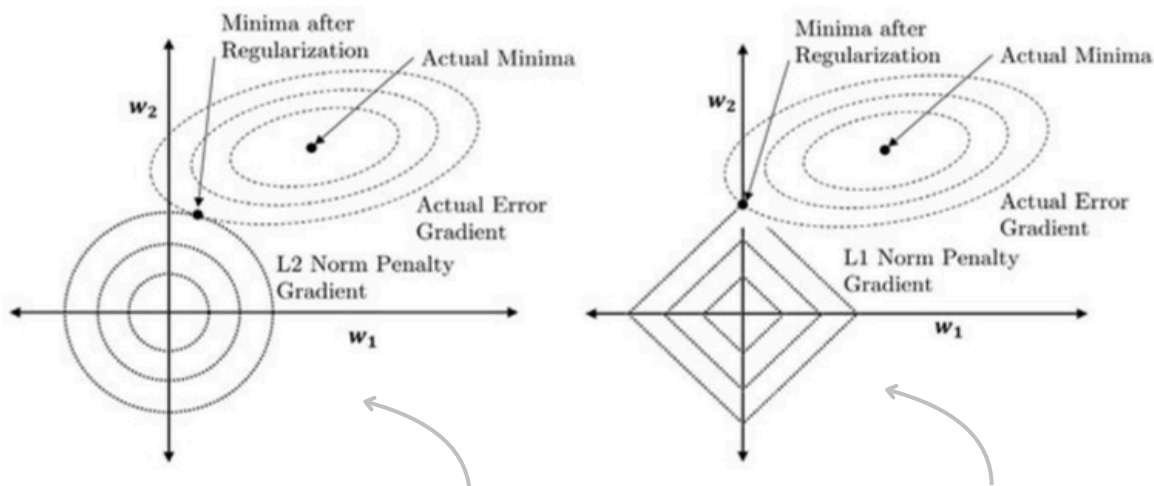
$$\mathbb{E} [D_R(f_{\alpha,N}^\delta, f^\dagger)] \lesssim N^{-1} \text{ for } \alpha \simeq N^{-1}.$$


Figure 1. Approximate decay of the expected value of the Bregman distance, with wavelets-based regularization, for $p = 3/2$ (left column) and $p = 4/3$ (right column). The phantom satisfies the strong source conditions. Top row: fixed noise regime. Bottom row: decreasing noise regime.

l1 , l2 regularization



feature	l2 regularization	l1 regularization
Penalty	Sum of squares	Sum of absolute values
Effect	Shrinks all coefficients	Promotes sparsity (many zeros)
Geometry	Circular constraint	Diamond-shaped constraint
Usage	Prevents overfitting (smooth models)	Feature selection (sparse models)

Conclusion

Convergence Rate

- If $\delta N \rightarrow \infty$ (and $\delta^2/N \rightarrow 0$), then

$$\mathbb{E} \left[D_{\tilde{R}}(f_{\alpha,N}^\delta, f^\dagger) \right] \lesssim \left(\frac{\delta^2}{N} \right)^{\frac{1}{3}} \text{ for } \alpha \simeq \left(\frac{\delta^2}{N} \right)^{\frac{1}{3}};$$

- If δN is bounded, then

$$\mathbb{E} \left[D_{\tilde{R}}(f_{\alpha,N}^\delta, f^\dagger) \right] \lesssim N^{-1} \text{ for } \alpha \simeq N^{-1}.$$

Table 1. Approximate decay of the expected value of the Bregman distance, with wavelets-based regularization, for $p = 3/2$ and $p = 4/3$.

Scenario	Theoretical	Strong source condition		Approx. source condition	
		$p = 3/2$	$p = 4/3$	$p = 3/2$	$p = 4/3$
Decreasing noise	-1	-1.0823	-1.0179	-1.0159	-1.023
Fixed noise	-1/3	-0.33043	-0.32503	-0.33152	-0.32659

Shearlet
regularization

Wavelet
regularization

Table 2. Approximate decay of the expected value of the Bregman distance, with shearlets-based regularization, for $p = 3/2$ and $p = 4/3$.

Scenario	Theoretical	$p = 3/2$	$p = 4/3$
Decreasing noise	-1	-1.1113	-1.0388
Fixed noise	-1/3	-0.33249	-0.32839

Limitations and potential Improvements

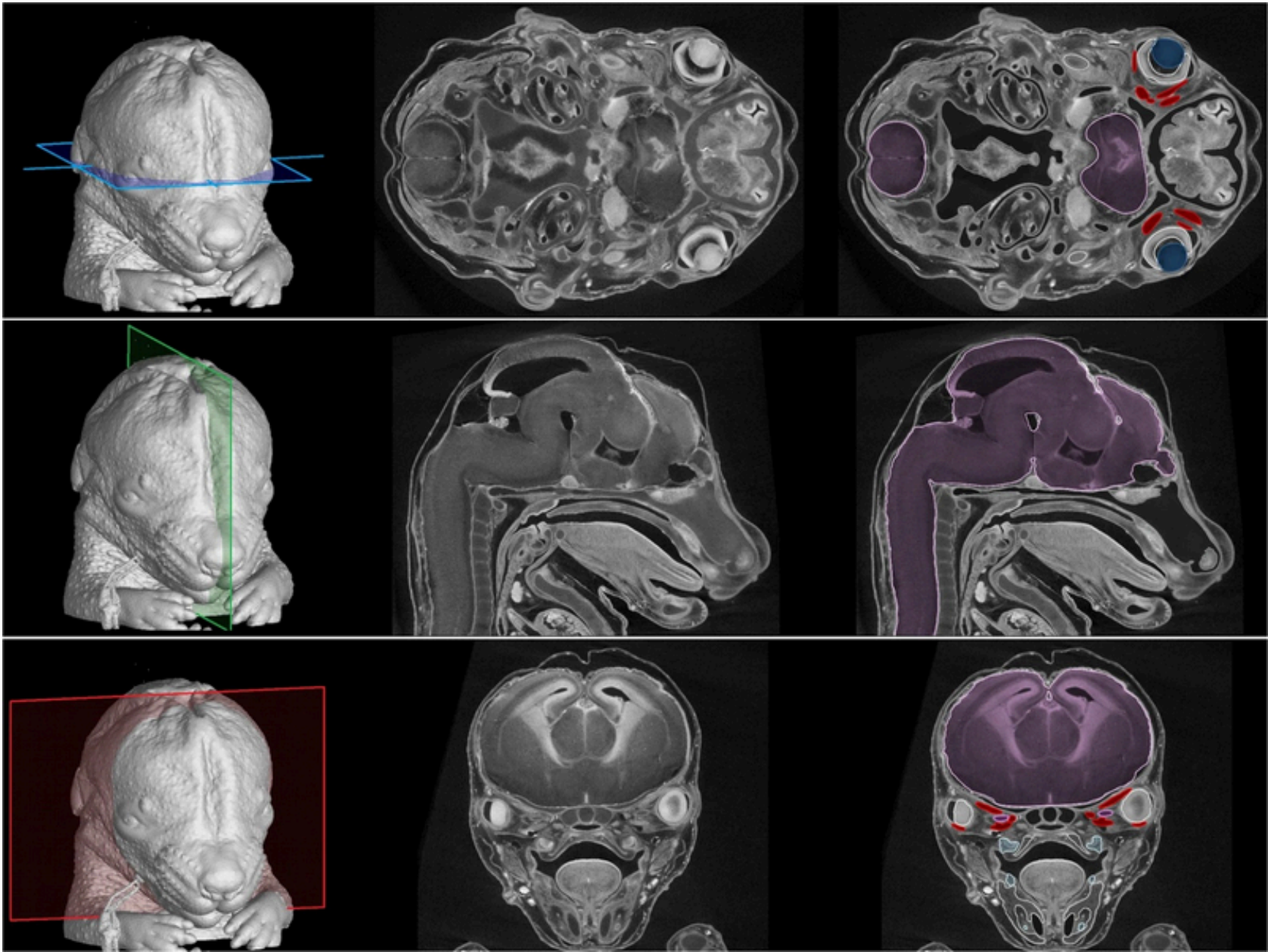
Noise Models and Practical Scenarios

- Performance with Mixed Noise (Gaussian + Salt-and-Pepper):
 - Shearlet methods may struggle with **salt-and-pepper noise** due to its outlier nature.
 - **Pre-processing techniques** (like robust denoising) or robust statistical methods may be needed for effective handling.
- Sensitivity to Noise Distribution:
 - Shearlets handle **Gaussian noise** well.
 - Performance can degrade with **non-Gaussian noise** (e.g., Poisson noise, in the case of low-light images).
 - **Modifications** or alternative regularization techniques may be required for different noise types.

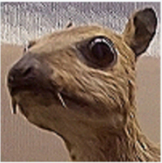

Non-negativity Constraints

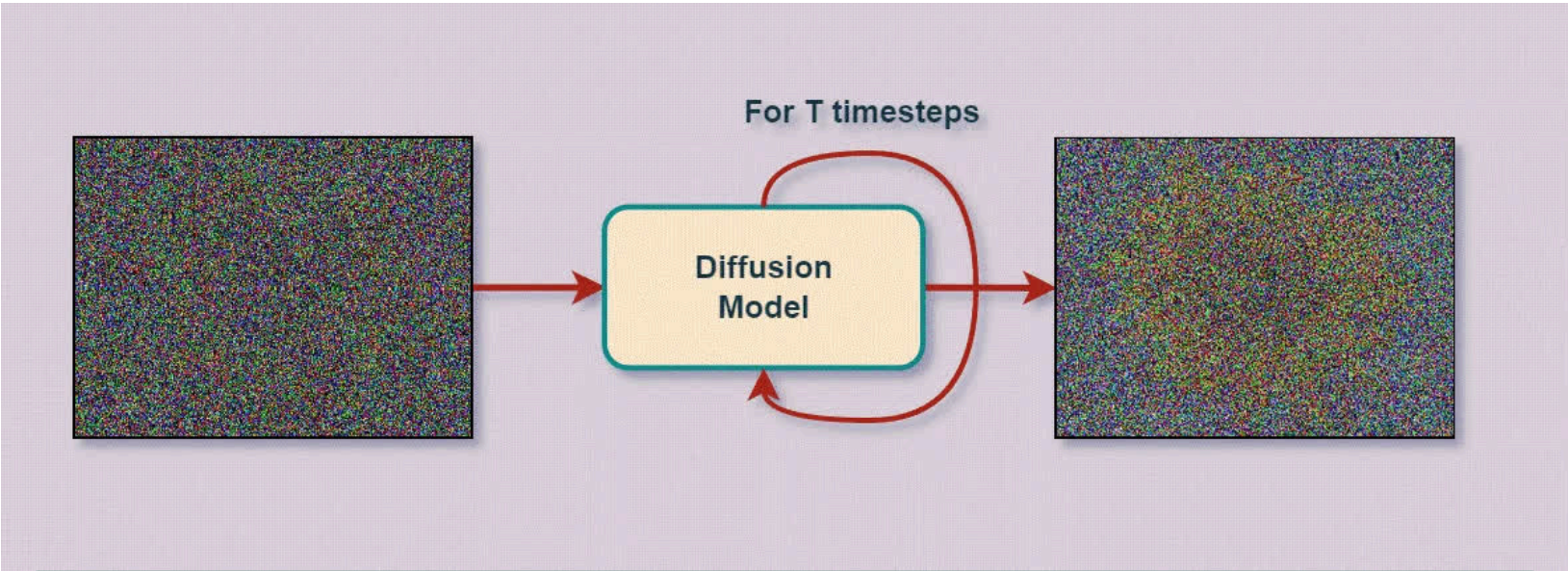
- Impact on Convergence:
 - Non-negativity constraints **slow down convergence** by adding restrictions.
 - However, they **enhance realism and physical interpretability** in imaging applications (e.g., X-ray tomography).

Reproducibility and comparison

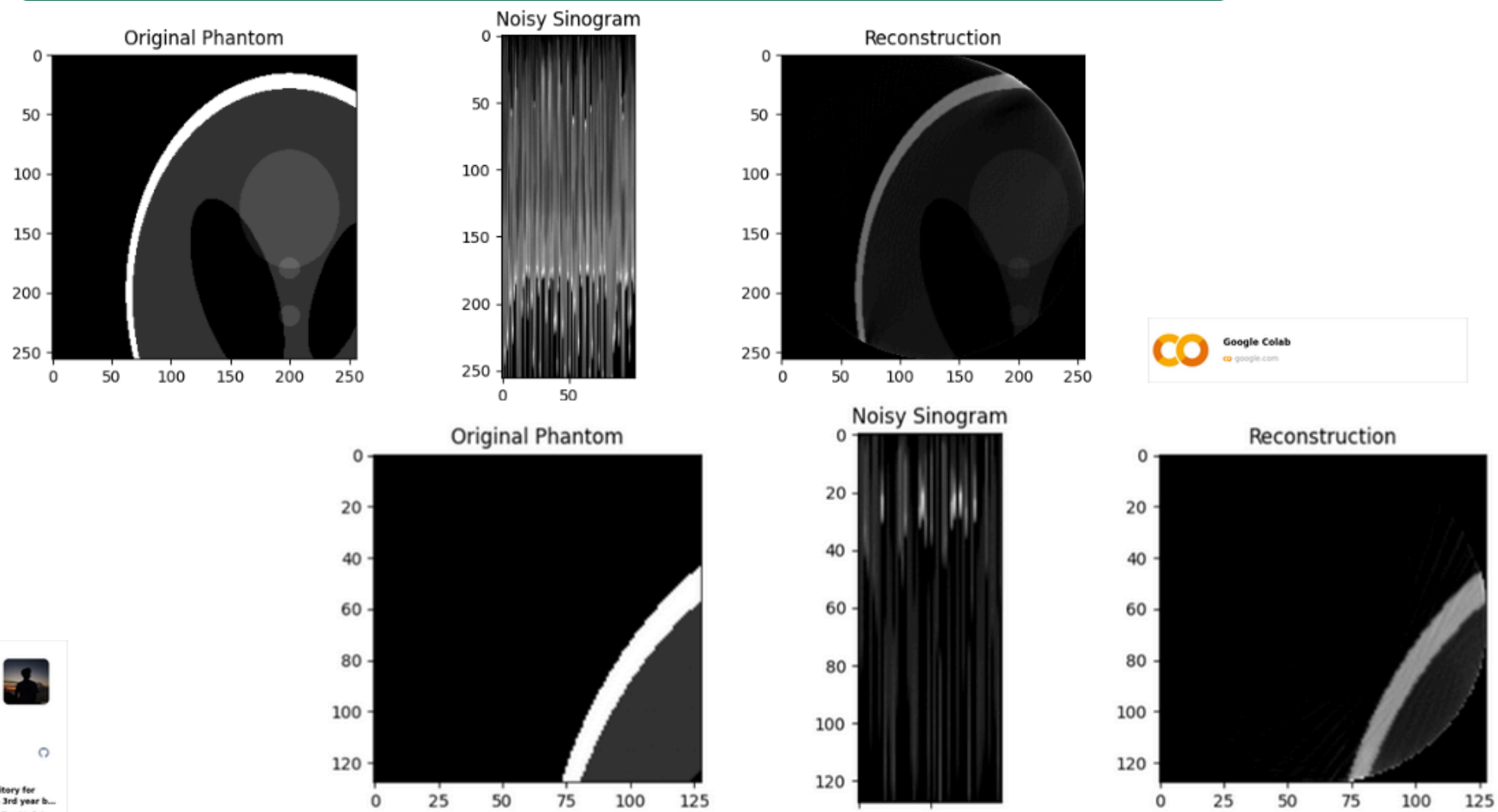


Computed Tomography Scans

Sharpen	$\begin{bmatrix} 0 & -1 & 0 \\ -1 & 5 & -1 \\ 0 & -1 & 0 \end{bmatrix}$	
Box blur (normalized)	$\frac{1}{9} \begin{bmatrix} 1 & 1 & 1 \\ 1 & 1 & 1 \\ 1 & 1 & 1 \end{bmatrix}$	



Diffusion Models



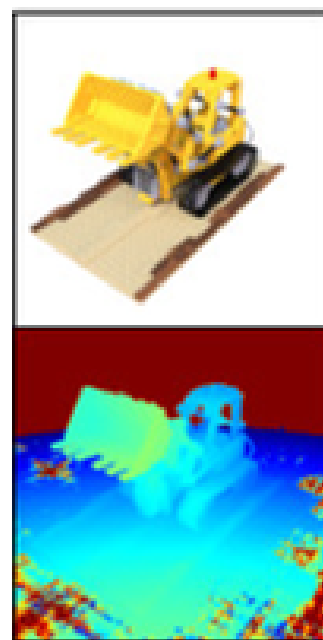
Deep Learning

Fine-grained Attribute Editing

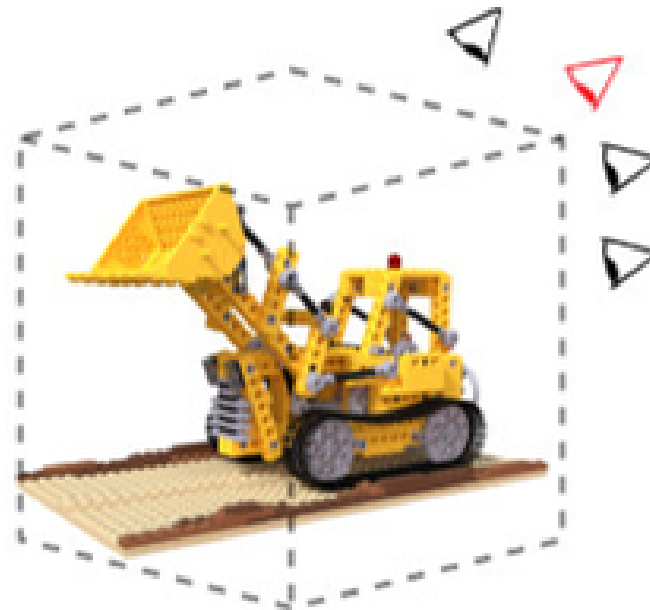


v1: Continuous **smile** control

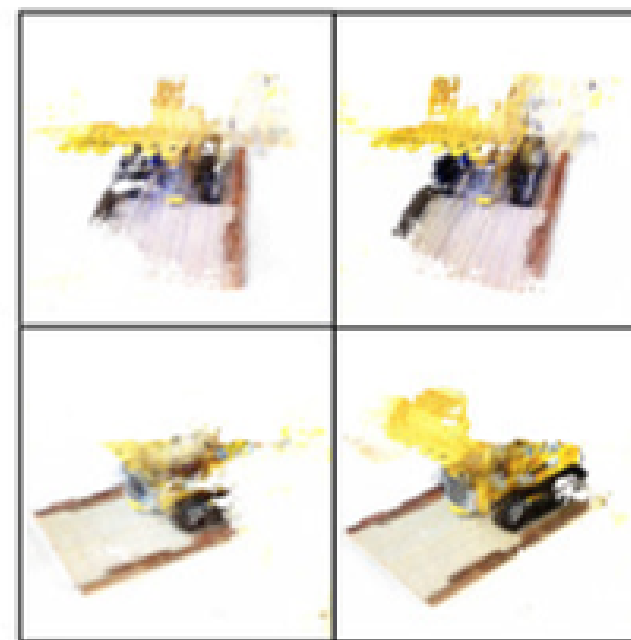
v2: Continuous **beard** control



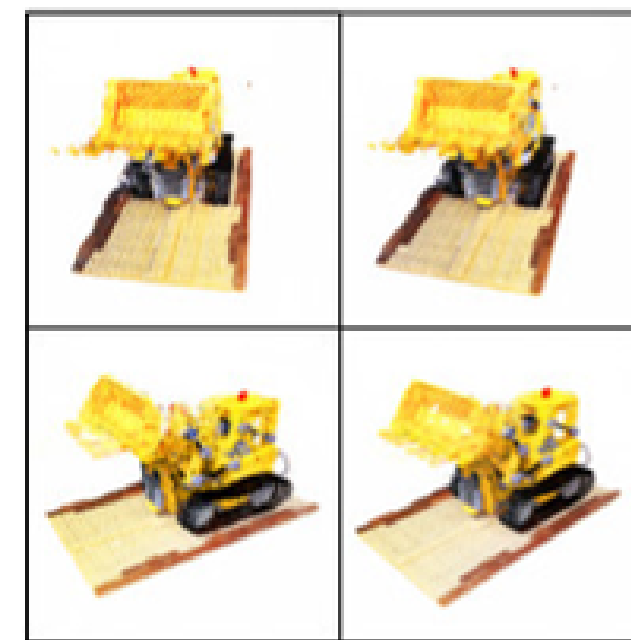
Reference



Neural Radiance Field



DS-NeRF



SinNeRF (Ours)

**Recent generative
State-of-the-Art
models used for
Image Reconstruction**

PreciseControl : Enhancing Text-to-Image Diffusion Models with Fine-Grained Attribute Control, Rishubh P. (ECCV, 24 [A*])
Representing Scenes as Neural Radiance Fields for View Synthesis (ECCV, 20[A*], Best paper)